Physics Letters A ••• (••••) •••–•••

Contents lists available at ScienceDirect

Physics Letters A

www.elsevier.com/locate/pla

Resonance, stability and period-doubling bifurcation of a quarter-car model excited by the road surface profile

M. Siewe Siewe *

Department of Mathematics and Applied Mathematics, University of Pretoria, Pretoria 0002, South Africa

ARTICLE INFO

Article history:
Received 20 November 2009
Received in revised form 15 January 2010
Accepted 21 January 2010
Available online xxxx
Communicated by A.R. Bishop

ABSTRACT

Stability and the steady states of the transverse motion of a quarter-car model excited by the road surface profile with non-symmetric potential is investigated. Initially, a set of slow-flow equations is derived using the method of multiple-time scales directly to the governing equation, governing the amplitudes and phases of approximate long time response of these oscillators, by applying an asymptotic analytical method. Determination of several possible types of steady-state motions is then reduced to solution of sets of algebraic equations. For all these solution types, appropriate stability analysis is also performed. In the second part of the study, this analysis is applied to an example mechanical system. First, a systematic search is performed, revealing effects of system parameters on the existence and stability properties of periodic motions. Frequency-response as well as forced-response diagrams are presented and attention is focused on understanding the evolution and interaction of the various solution branches as the external forcing and nonlinearity parameters are varied. Finally, numerical integration of the equations of motion demonstrates that the system exhibits period-doubling bifurcation or chaotic response for some parameter combinations.

1. Introduction

The study on response and stability of nonlinear system has been investigated by many investigators mainly using the perturbation technique [1–3] due to the fact that a lot of problems in engineering and practical science can be modelled as a nonlinear system. Sometimes the application of a small force to mechanical system causes a considerable growth in the amplitude of a stable oscillations. The resulting large-amplitude vibrations are a problem in many engineering applications. A familiar example is a pushed playground swing: (smoothly) pushing a swing (almost) in tune with its natural frequency will make the swing's amplitude increase to some maximal amplitude oscillation, commonly known as a resonance oscillation.

Hysteretic nonlinear suspension system induced oscillation under various form of external excitation is a widely studied fundamental mechanics problem by many researchers. Theoretical models of chaotic response of quarter-car models due to nonlinear stochastic and deterministic excitation have been developed and have been experimentally observed due to the excitation of the road profile [4–9]. These previous related works have been limited to conventional chaotic motion of a quarter car and have not attacked primary, subharmonic and superharmonic resonances at all. In Ref. [5], the authors investigated numerically and analytically by using a method of harmonic balance the principal resonances for different shapes of the restore force potential. In Ref. [8], the authors analyzed the transition to chaos as in [6] by treating the gravity force as a perturbation in the Melnikov function. In this letter, we focus on this issue.

The main objective of the present study is the influence of the road profile on the entrainment area of the primary, subharmonic and superharmonic resonance, and their stability for a one-degree of freedom excited oscillator for Rayleigh–Duffing type that can be used to model quarter-car motion. Emphasis is placed on the effects caused by the one to-one, three to-one and one to-three resonance. Stability analysis and numerical simulation studies of subharmonic resonances in various types of harmonically excited one-degree of freedom excited oscillators have shown that chaotic motions are associated with the loss of stability of a subharmonic or superharmonic resonance, i.e. one characteristic precursor to chaotic motions is the appearance and then loss of stability of a subharmonic or superharmonic resonance, e.g. Refs. [10–13].

For this case, the method of multiple time scales is applied first, yielding a set of slow-flow equations for the amplitudes and phases of approximate motions of the system. The stability analysis of these motions is also performed. Then, numerical results are presented in the form of response diagrams, by solving the

* Permanent address: Université de Yaoundé I, Faculté des sciences, Département de Physique, Laboratoire de Mécanique, BP: 812 Yaoundé, Cameroun.
E-mail addresses: martinsiewesiewe@yahoo.fr, martin.siewe@up.ac.za.

0375-9601/$ – see front matter
doi:10.1016/j.physleta.2010.01.043

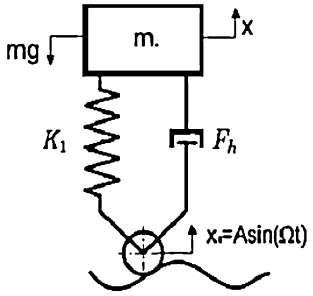

Fig. 1. Model of quarter car subjected to a kinematic excitation.

slow-flow equations for constant solutions. Attention is focused on understanding the changes that occur in the response by varying the value of certain system parameters. In addition, results obtained by direct integration of the equations of motion are presented, showing the existence of some other, more complicated types of response. The final section summarizes the most important findings of the study.

2. Description of the mathematical model

The goal of this part is to describe the simplified model which will be the subject of our work and will establish the equation of the movement which governs its dynamics. The model of the quarter car (see [6]) is represented on Fig. 1. It consists of a block of mass m, a spring with a constant stiffness k_1 whose stiffness force is defined by

$$k_1(x-x_0), \tag{1}$$

where $(x-x_0)$ is a relative displacement of the spring forces, k_1 is the linear spring constant. Only the movement of pumping describes by the co-ordinate x and which is recalled to its initial position by the spring constant k_1 fixed between the wheel and the block is considered. In addition the model has between the wheel and the block a shock absorber whose force of friction is given by Li et al. [4]

$$F_h\left(\frac{d}{dt}(x-x_0),(x-x_0)\right) = k_2(x-x_0)^3 + C_1\frac{d}{dt}(x-x_0) + C_2\left(\frac{d}{dt}(x-x_0)\right)^3, \tag{2}$$

where F_h is an additional nonlinear hysteretic suspension damping and stiffness force dependent on relative displacement and velocity. The block-arise-shock absorber–wheel unit circulates on a sinuous road whose position of the wheel compared to the surface part of the road is given by the following expression

$$x_0 = A\sin(\Omega t), \tag{3}$$

where x_0 is a reference position of the wheel which varies according to the highway type and A the maximum amplitude of the road. For an ideal road, the amplitude A is identically zero. To establish the equation governing the dynamics of the system, we are used the second law of Newton which leads to

$$m\frac{d^2x}{dt^2} + k_1(x-x_0) + k_2(x-x_0)^3 + C_1\frac{d}{dt}(x-x_0) + C_2\left(\frac{d}{dt}(x-x_0)\right)^3 + mg = 0. \tag{4}$$

Defining a new variable for a relative displacement as $y = x - x_0$ we get

$$\frac{d^2y}{dt^2} + w^2y + B_1y^3 + B_2\frac{dy}{dt} + B_3\left(\frac{dy}{dt}\right)^3 = -g + A\Omega^2\sin(\Omega t), \tag{5}$$

where $w^2 = \frac{k_1}{m}$, $B_1 = \frac{k_2}{m}$, $B_2 = \frac{C_1}{m}$, $B_3 = \frac{C_2}{m}$. The corresponding dimensionless equation of motion can be written for a scaled time variable $\tau = wt$ as:

$$\ddot{y} + y + ky^3 + \alpha\dot{y} + \beta\dot{y}^3 = -g' + A\Omega'^2\sin(\Omega' t), \tag{6}$$

where

$$k = \frac{k_2}{k_1}, \qquad \alpha = \frac{C_1}{\sqrt{k_1 m}}, \qquad \beta = C_2\sqrt{\frac{k_1}{m^3}}, \qquad g' = \frac{g}{w^2}, \qquad \Omega' = \frac{\Omega}{w}. \tag{7}$$

Following Li et al. [4], the system parameters are defined as:

$$m = 240\ \text{kg}, \qquad k_1 = 160\,000\ \text{N/m}, \qquad k_2 = -300\,000\ \text{N/m}^3, \qquad C_1 = -250\ \text{Ns/m}, \qquad C_2 = 25\ \text{Ns}^3/m^3.$$

The corresponding asymmetry potential is defined by

$$V(y) = g'y + \frac{1}{2}y^2 + \frac{1}{4}ky^4. \tag{8}$$

3. Local bifurcation analysis

In this section, we shall give the local bifurcation analysis for Eq. (6). The analysis is based on the averaged Eq. (6), which will be obtained using the method of multiple-time scales [1–3]. To start with, one assumes that a uniform solution of Eq. (6) can be represented in the form

$$y(t,\varepsilon) = y_0(T_0,T_1) + \varepsilon y_1(T_0,T_1) + \cdots, \tag{9}$$

where $T_0 = t$ and $T_1 = \varepsilon t$. Note that a general solution (9) given on the form of multiple scales should include unlimited time scales $T_0, T_1, T_2, \ldots$. Here we only take two scales T_0 and T_1, which are usually called two time scales, because it is enough for the analysis of Eq. (6). Suppose k, α, β to be small parameters that is $k = \varepsilon k$; $\alpha = \varepsilon\alpha$; $\beta = \varepsilon\beta$ where ε is a small perturbation parameter, then, the differential operators become

$$\frac{d}{dt} = D_0 + \varepsilon D_1 + \cdots, \qquad \frac{d^2}{dt^2} = D_0^2 + 2\varepsilon D_0D_1 + \cdots, \tag{10}$$

where $D_n = \frac{\partial}{\partial T_n}$, $T_n = \varepsilon^n$, $n = 0, 1$.

3.1. The nonresonant case

In this case, we suppose that Ω' is away from ω_0. The effect of the excitation will be small unless its amplitude is hard [2]; as in the case of the primary resonances, we seek an approximate solution by using multiple time scales method. Substituting Eqs. (9) and (10) into Eq. (6) and equating the coefficients of like power of ε on both sides, we obtain order ε^0,

$$D_0^2y_0 + y_0 = -g' + F_0\sin\Omega'\tau, \tag{11}$$

order ε^1,

$$D_0^2y_1 + y_1 = -2D_0D_1y_0 - ky_0^3 - \alpha D_0y_0 - \beta(D_0y_0)^3. \tag{12}$$

The general solution of the first equation of system (11) can be written now as

$$y_0 = A(T_1)\exp jT_0 + B\exp j\left(\Omega' T_0 - \frac{\pi}{2}\right) - \frac{1}{2}g' + c.c., \tag{13}$$

where *c.c.* stands for the complex conjugate of the preceding terms, where $B = \frac{F_0}{2(1-\Omega'^2)}$, and $A(T_1)$ is undefined function at this step. Substituting Eq. (13) into Eq. (12), one obtain

$$\begin{aligned} D_0^2 y_1 + y_1 = {} & \left(-2j\dot{A} - j\alpha A - 3k|A|^2 A\right)\exp j\Omega' T_0 \\ & - \left(6kAB^2 + 3j\beta|A|^2 A\right)\exp jT_0 \\ & - \left(6j\beta A\Omega'^2 B^2 + 3kAg'^2\right)\exp jT_0 \\ & - B\left(\alpha\Omega' - 6jk|A|^2 - 3jkB^2\right)\exp j\Omega' T_0 \\ & - B\left(6\beta|A|^2\Omega' + 3\beta\Omega'^3 B^2 - 3jkg'^2\right)\exp j\Omega' T_0 \\ & - 3AB^2\left(k - j\beta\Omega'^2\right)\exp j\left(\left(1+2\Omega'\right)T_0 - \pi\right) \\ & + A^3(-k + j\beta)\exp 3jT_0 \\ & - B^3\left(jk + \beta\Omega'^3\right)\exp 3j\Omega' T_0 \\ & - 3AB^2\left(k - j\beta\Omega'^2\right)\exp j\left(\left(1-2\Omega'\right)T_0 + \pi\right) \\ & - 3A^2 B\left(jk - \beta\Omega'\right)\exp\left(2+\Omega'\right)T_0 \\ & - 3A^2 B\left(jk - \beta\Omega'\right)\exp j\left(2-\Omega'\right)T_0 \\ & + 3kA^2 g'\exp 2jT_0 - 3jg'kB^2\exp 2j\Omega' T_0 \\ & + 6jABg'k\exp j\left(\Omega'+1\right)T_0 \\ & + 6jABg'k\exp j\left(1-\Omega'\right)T_0 - \frac{1}{2}kg'^3 + c.c. \end{aligned} \tag{14}$$

From Eq. (14), secular terms may occur whenever $\Omega' = 0(\varepsilon)$ or whenever there is a secondary resonance, that is, whenever $3\Omega' = 1$, $2\Omega' = 1$, $\Omega' = 3$ or $\Omega' = 2$. The cases $3\Omega' = 1$, $2\Omega' = 1$ are called superharmonic resonances and the second cases $\Omega' = 3$ or $\Omega' = 2$ are called subharmonic resonances. In the nonresonant case secular terms are eliminated if

$$\begin{aligned} & 2j\dot{A} + j\alpha A + 3k\left(|A|^2 + 2B^2\right)A + 3j\beta\left(|A|^2 + 2\Omega'^2 B^2\right)A \\ & \quad + 3kAg'^2 = 0, \end{aligned} \tag{15}$$

expressing $A(T_1)$ in the polar form as follows

$$A(T_1) = \frac{1}{2}a(T_1)\exp jb(T_1), \tag{16}$$

and inserting in Eq. (15) we thus obtain the following set of first order differential equations for the amplitude and phase:

$$\begin{cases} \dot{a} = -a\left(\frac{1}{2}\alpha + \frac{3}{2}\beta\left(\frac{1}{4}a^2 + 2\Omega'^2 B^2\right)\right), \\ \dot{b} = \frac{3}{2}k\left(\frac{1}{4}a^2 + 2B^2 + g'^2\right). \end{cases} \tag{17}$$

When $k = 0$, we have oscillations if the phase is constant and different from zero. If $k \neq 0$ the phase b is no more a constant, but the oscillations exists. In its general form, the first equation in system Eq. (17) shows that in the nonresonant case, the time evolution of the amplitude is given by

$$a(T_1) = \sqrt{\frac{a_1}{(a_0\exp(-2\lambda T_1) - 1)}}, \tag{18}$$

in with $a_1 = \frac{-8\lambda}{3\beta}$, $\lambda = -(\frac{\alpha}{2} + 3\beta\Omega'^2 B^2)$ and a_0 the initial amplitude. The phase is defined by

$$b(T_1) = b_1 \ln b_0\left(a_0 - \exp(\lambda T_1)\right) + g'' T_1, \tag{19}$$

where $b_1 = \frac{k}{2\beta}$, $g'' = \frac{3kg'^2}{2} + 3kB^2$ and b_0 is the initial phase.

When $\lambda < 0$ (i.e. $\alpha > 6\beta\Omega'^2 B^2$), then $a \to 0$ when $T_1 \to \infty$ and the steady state is periodic, consisting of the forced solution only.

When $\lambda > 0$ (i.e. $\alpha < 6\beta\Omega'^2 B^2$), the oscillator amplitude $a \to \sqrt{\frac{8\lambda}{3\beta}}$ when $T_1 \to \infty$ and the steady-state motion consists of combination of the forced and free solutions; in this case there is no periodic motion.

3.2. The primary resonance case ($\Omega' = 1 + \varepsilon\sigma$)

To find the amplitude of the oscillations at the primary resonance, we assume that $F_0 = \varepsilon F_0$. Substituting Eqs. (9) and (10) into Eq. (6) and equating coefficients of like powers of ε leads to the following differentials equations

$$D_0^2 y_0 + y_0 = -g', \tag{20}$$

$$\begin{aligned} D_0^2 y_1 + y_1 = {} & -2D_0 D_1 y_0 - k y_0^3 - \alpha D_0 y_0 - \beta(D_0 y_0)^3 \\ & + F_0\sin(T_0 + \sigma T_1) + c.c. \end{aligned} \tag{21}$$

The general solution of Eq. (20) is given by:

$$y_0 = A(T_1)\exp(jT_0) - \frac{1}{2}g' + c.c. \tag{22}$$

Substituting the expression of y_0 into Eq. (21), the condition for eliminating secular terms is given by:

$$\begin{aligned} & -2j\dot{A} - j\alpha A - 3\beta j|A|^2 A - 3k|A|^2 A \\ & \quad + \frac{1}{2}F_0\exp j\left(\sigma T_1 - \frac{\pi}{2}\right) - 3kAg'^2 = 0. \end{aligned} \tag{23}$$

We seek the solution of Eq. (23) in the polar form given in Eq. (16). We thus obtain after separating real and imaginary parts the following set of coupled nonlinear first order differential equations for the amplitude and phase:

$$\begin{cases} \dot{a} = -\frac{\alpha}{2}a - \frac{3\beta}{8}a^3 + \frac{1}{2}F_0\sin\delta, \\ a\dot{\delta} = a\sigma - \frac{3k}{8}a^3 - \frac{3kg'^2}{2}a + \frac{1}{2}F_0\cos\delta, \end{cases} \tag{24}$$

where $\delta = \sigma T_1 - b - \frac{\pi}{2}$. The steady-state motions correspond to $\delta = \sigma T_1 - b - \frac{\pi}{2}$. Then eliminating δ from Eq. (10) we obtain the following nonlinear algebraic equation for steady state at the primary resonance

$$\left(a_0\sigma - \frac{3k}{8}a_0^3 - \frac{3kg'^2}{2}a_0\right)^2 + \left(\frac{3\beta}{8}a_0^3 + \frac{\alpha}{2}a_0\right)^2 = \frac{1}{4}F_0^2. \tag{25}$$

The analytical resolution of Eq. (25) being complex, we will use a numerical resolution based on the Newton–Raphson's algorithm. We present the sweeping in frequency of forcing σ for various values of F_0 Fig. 2(a), and the sweeping in amplitude of forcing F_0 for various values of σ Fig. 2(b). It appears that the curves of resonance slightly tilted to the left side like are planned for a nonlinear system with constant of stiffness $k(< 0)$ Fig. 2(a) implying the presence of the hysteresis phenomenon. The amplitude of the resonance monotonic decreasing function of the road profile excitation amplitude F_0. For the sweeping in amplitude of forcing, we note the gap of curve towards the large amplitudes when F_0 grows Fig. 2(b).

The result of the stationary state given by relation (25) has a physical sense if and only if it is stable. The stability of each fixed point (a_0, δ_0), where a_0 and δ_0 are the value of a and δ in the stationary state can be determined by using the method of Andronov and Vitt [14]. To this purpose let us assume that singular point is subjected to small perturbations characterized by slight variation of a and δ. That is,

$$a = a_0 + a_1, \qquad \delta = \delta_0 + \delta_1. \tag{26}$$

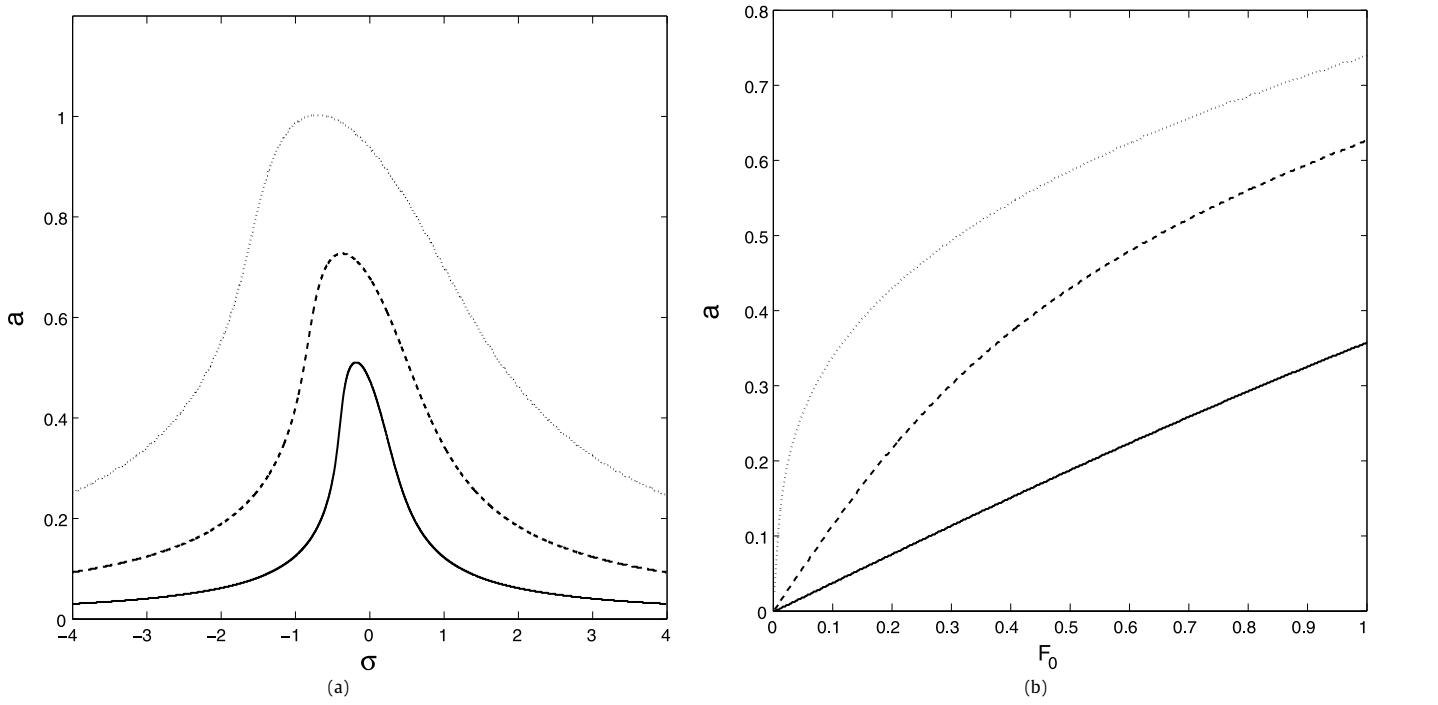

Fig. 2. (a) Frequency response curve response for different excitation amplitude: $F_0 = 0.25$ (solid line), $F_0 = 0.75$ (dash line), $F_0 = 2$ (dot line). (b) Forced response curve for different values of detuning parameter: $\sigma = 1.3$ (solid line), $\sigma = 0.425$ (dash line), $\sigma = 0.03$ (dot line).

Substituting Eq. (26) into Eq. (24) and keeping only the linear terms in a_1 and δ_1, we obtain

$$\begin{cases} \dot{a}_1 = -\left(\dfrac{\alpha}{2} + \dfrac{9\beta a_0^2}{4}\right)a_1 + \left(\dfrac{3kg^2}{2}a_0 - \sigma a_0 + \dfrac{3k}{8}a_0^3\right)\delta_1, \\ \dot{\delta}_1 = \dfrac{1}{a_0}\left(\sigma - \dfrac{3kg^2}{2} - \dfrac{9ka_0^2}{8}\right)a_1 - \left(\dfrac{\alpha}{2} + \dfrac{3\beta a_0^2}{8}\right)\delta_1. \end{cases} \tag{27}$$

Thus the steady-state solutions are stable if the eigenvalues ξ of the coefficient matrix of the right-hand sides of Eq. (27) all have their real parts negative. These eigenvalues are characterized by the algebraic equation

$$\xi^2 + 2P\xi + Q = 0, \tag{28}$$

where

$$P = 2\alpha + 3\beta a_0^2 \tag{29}$$

and

$$Q = \left(\frac{\alpha}{2} + \frac{9\beta a_0^2}{4}\right)\left(\frac{\alpha}{2} + \frac{3\beta a_0^2}{8}\right) + \left(\sigma - \frac{3kg^2}{2} - \frac{3k}{8}a_0^2\right)\left(\sigma - \frac{3kg^2}{2} - \frac{9ka_0^2}{8}\right). \tag{30}$$

Hence if $P > 0$ the steady-state solutions are unstable for $Q < 0$. When $P < 0$ all the steady-state solutions are unstable. Fig. 3 presents the amplitudes response curves for different values of the external excitation and the unstable and stable domain in the (a_0, σ). The white domain corresponds to stable solutions while the shaded domain represents the unstable solutions domain.

3.3. Subharmonic and superharmonic resonances

This types of oscillations appear in the system when the amplitude of the external excitation is large. For our model oscillator,

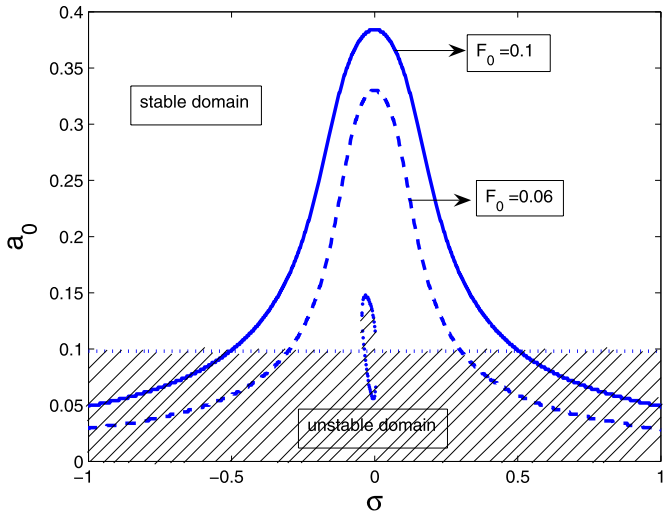

Fig. 3. Stable and unstable domains in the parameter space.

as described in the precedent section, there exist two case of subharmonic and superharmonic resonance in the system: the third and the second secondary resonance. In this section we treat only the case of the superharmonic state $3\Omega' = 1$ and the subharmonic state $\Omega' = 3$. In a similar way the amplitudes of the third secondary resonance can be found.

For the superharmonic state $3\Omega' = 1 + \varepsilon\sigma$, the amplitude and the stability of the resonance state can be obtained using the procedure described above for the primary resonance with the expression of y_0 given by Eq. (13). In this case the resonance equation is governed by

$$\left[\frac{1}{2}a_0\left(\alpha + \frac{3}{4}\beta a_0^2\right) - 3\beta a_0 \Omega'^2 B^2\right]^2 - \left(\beta\Omega'^3 B^3\right)^2 = -\left[\sigma a_0 - 3ka_0\left(\frac{1}{8}a_0^2 + B^2\right) - \frac{3}{2}kg'^2 a_0\right]^2 + \left(kB^3\right)^2. \tag{31}$$

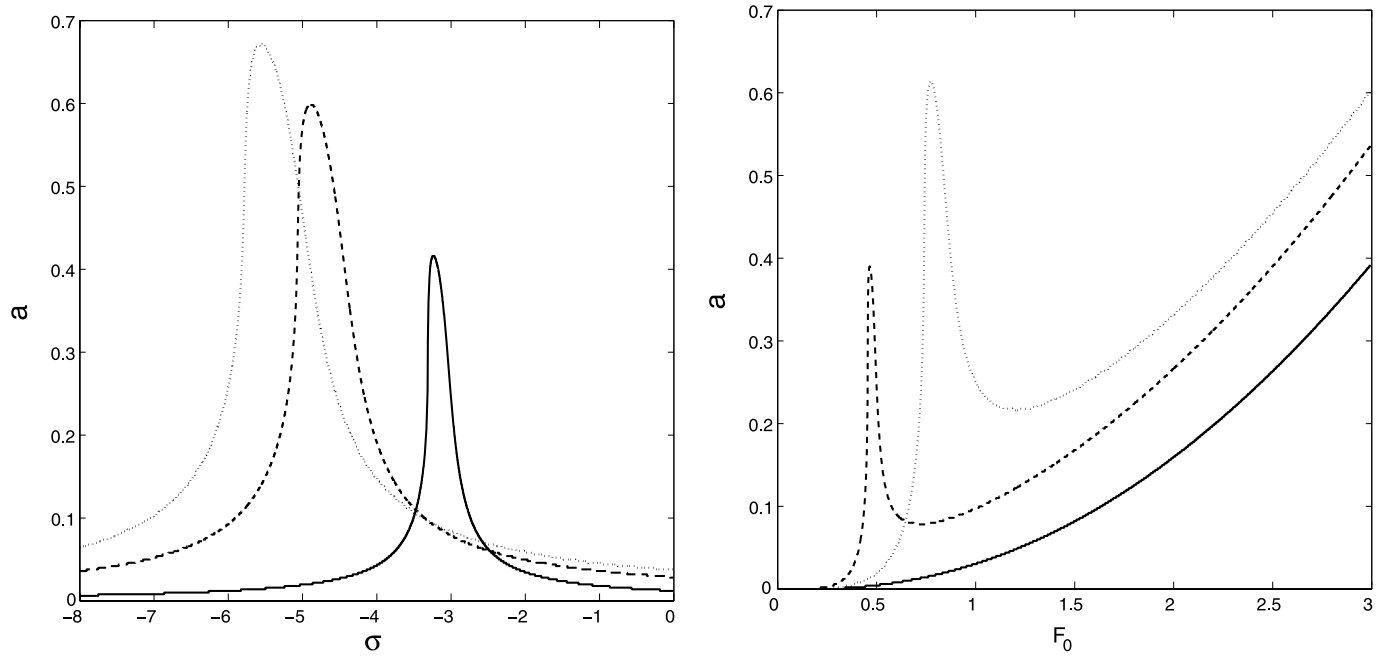

(a) (b)

Fig. 4. (a) Frequency response curve response for different excitation amplitude in the case of superharmonic resonance with $\varepsilon = 0.02$: $F_0 = 0.5$ (solid line), $F_0 = 0.75$ (dash line), $F_0 = 0.85$ (dot line). (b) Forced response curve for different values of detuning parameter: $\sigma = 5$ (solid line), $\sigma = -3$ (dash line), $\sigma = -5$ (dot line).

Thus, in the case of superharmonic resonance the vertical displacement of the quarter of vehicle is given by

$$y(t) = a_0 \cos\left(3\Omega' t + \delta\right) + B\cos\left(\Omega' t\right) + \vartheta(\varepsilon), \tag{32}$$

thus, the steady-state solutions given by Eq. (31) will be physically stable if the eigenvalues ξ of the following equation

$$\xi^2 + 2P\xi + Q = 0, \tag{33}$$

where

$$P = \frac{1}{2}\left(\alpha + 6\beta\Omega^2 B^2 + \frac{3\beta}{2}a_0^2\right) \tag{34}$$

and

$$\begin{aligned} Q = {} & \left(\frac{\alpha}{2} + 3\beta\Omega^2 B^2 + \frac{3\beta}{8}a_0^2\right)\left(\frac{\alpha}{2} + 3\beta\Omega^2 B^2 + \frac{9\beta}{8}a_0^2\right) \\ & + \left(\sigma - \frac{3kg^2}{2} - 3kB^2 - \frac{9k}{8}a_0^2\right) \\ & \times \left(\sigma - \frac{3kg^2}{2} - 3kB^2 - \frac{3ka_0^2}{8}\right). \end{aligned} \tag{35}$$

Hence if $P > 0$ the steady-state solutions are unstable for $Q < 0$. When $P < 0$ all the steady-state solutions are unstable. In order to illustrate the effects of the amplitude of the excitation of the external force, and the detuning parameter, we have plotted the amplitude a versus σ in Fig. 4(a) and a versus F_0 in Fig. 4(b). Fig. 4(a) indicates a shift of frequency response from the right to the left with the increases of the peak of the resonance as the amplitude of the external excitation increase. In Fig. 4(b), one can see the formation of resonance and antiresonance as the detuning parameter decreases, there also a shift of the forced response when varying the detuning parameter.

For the subharmonic resonance $\Omega' = 3 + \varepsilon\sigma$, the amplitudes are given by

$$\begin{aligned} & \left(\frac{1}{2}\alpha + \frac{3}{8}\beta a_0^2 + 3\beta\Omega'^2 B^2\right)^2 + \left(\frac{1}{3}\sigma - \frac{3}{8}ka_0^2 - \frac{3}{2}kg'^2 - 3kB^2\right)^2 \\ & = \left(\frac{3}{4}\beta\Omega' B a_0\right)^2 + \left(\frac{3}{4}ka_0 B\right)^2. \end{aligned} \tag{36}$$

Thus, in the case of the subharmonic resonance, the displacement of the quarter car is described by the following equation:

$$y(t) = a_0 \cos\left(\frac{1}{3}\Omega' t + \delta\right) + B\cos\Omega' t + \vartheta(\varepsilon). \tag{37}$$

In a similar way, one can find the amplitudes and the stability of the third subharmonic and superharmonic resonances. The instability boundaries are obtain when

$$P = \frac{1}{2}\left(\alpha + 6\beta\Omega^2 B^2 + \frac{3\beta}{2}a_0^2\right) \tag{38}$$

and

$$\begin{aligned} Q = {} & -3\left(\frac{\alpha}{2} + 3\beta\Omega^2 B^2 - \frac{3\beta}{8}a_0^2\right)\left(\frac{\alpha}{2} + 3\beta\Omega^2 B^2 + \frac{3\beta}{8}a_0^2\right) \\ & - 3\left(\frac{\sigma}{3} + \frac{3kg^2}{2} + 3kB^2 - \frac{3k}{8}a_0^2\right)\left(\frac{3kg^2}{2} + 3kB^2 + \frac{3ka_0^2}{4}\right). \end{aligned} \tag{39}$$

The amplitude response a versus σ for $F_0 = 0.15$ is plotted in Fig. 5(a), and the forced amplitude, i.e. a versus F_0 for $\sigma = 0.25$ is also plotted in Fig. 5(b). These two figures illustrate essentially an isola of period-1 solution. In Fig. 5(a), the isola of limit cycles is born in a saddle-node bifurcation near the detuning parameter of $\sigma = 0.257$. The dashed line indicates the limit cycle is unstable. The same phenomenon appears in Fig. 5(b) but the isola of limit cycles is born in a saddle-node bifurcation near the amplitude forcing parameter of $F_0 = 0.122$. Here, we note that although the frequency of the excitation is three times the natural frequency of the quarter car, the subharmonic response is quite large.

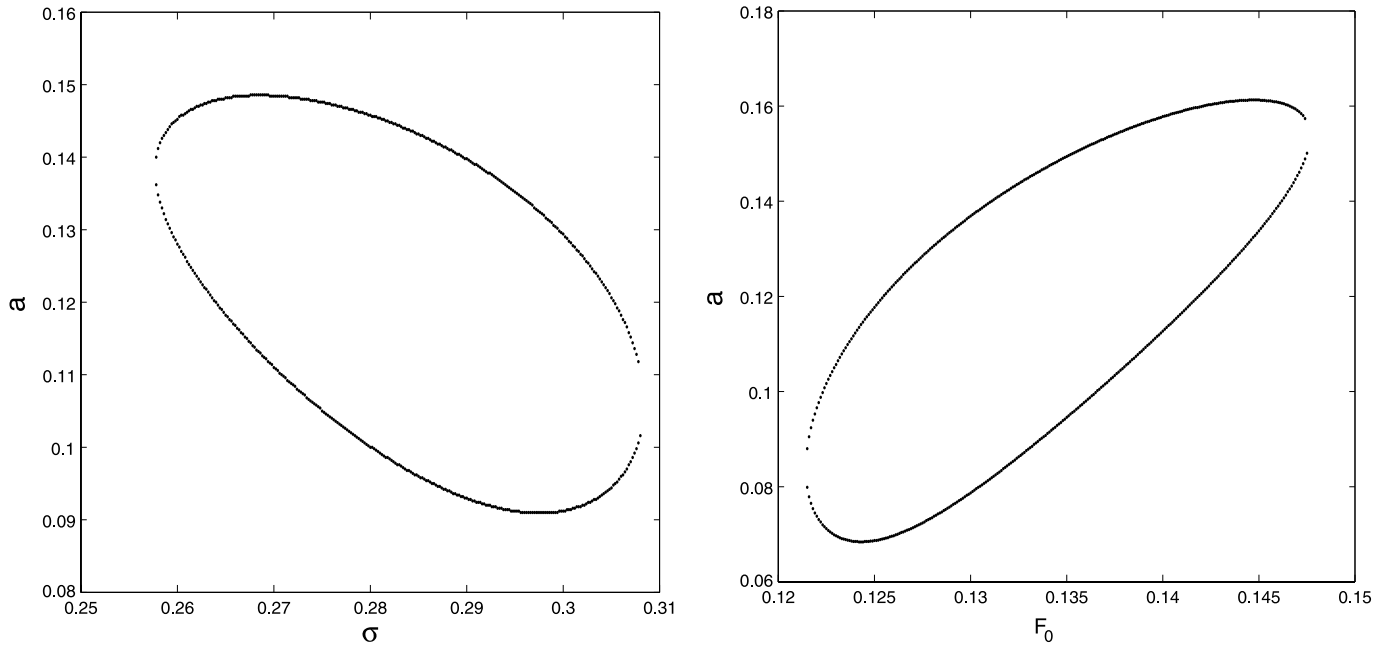

(a) (b)

Fig. 5. (a) Frequency response of subharmonic resonance for $\varepsilon = 0.02$, $F_0 = 0.15$. (b) Forced response of subharmonic resonance for $\varepsilon = 0.02$, $\sigma = 0.25$.

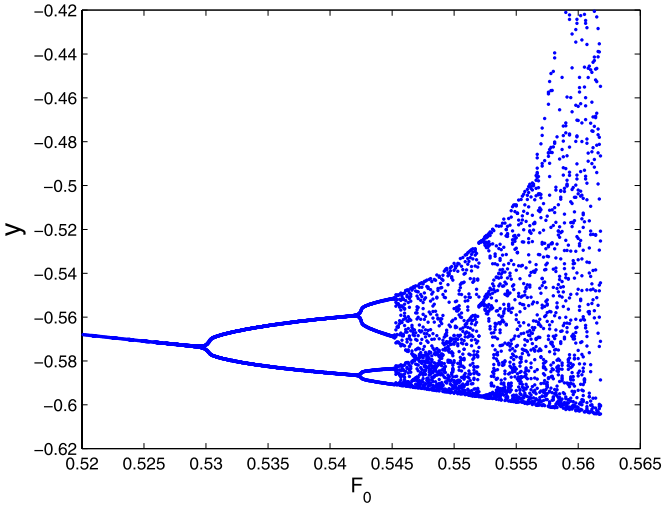

Fig. 6. Bifurcation diagram for the frequency parameter $\Omega' = 1$.

4. Numerical simulation and chaotic motion

The aim of this section is to use numerical analysis to establish parameter regimes where specific behavior could be expected, and thus to determine for which parameter combinations either periodic, quasi-periodic or chaotic behavior could be avoided or encountered. The diagnostics used to establish structural changes involved, bifurcation diagrams in the intervals of the amplitude of the external forcing F_0 and the influence of F_0 in the phase portrait diagram. The fourth-order Runge–Kutta routine is used for numerical integration of the model (6) under the initial condition $(y_0, \dot{y}_0) = (0, 0.1)$ and the external frequency of the road excitation $\Omega' = 1$. The bifurcation diagrams for specific parameter values are presented in Fig. 6 showing the sequence of period doubling route to chaos. It is notice that the system is fundamentally periodic and there is a single period-1 solution persisting for $F_0 < 0.53$. At the value of $F_0 = 0.53$, a period-2 solution is born and as F_0 increases the system undergoes a second period doubling giving rise to a period-4 solution and after to chaotic attractor as shown in Fig. 6. A chaotic-saddle explosion appears at $F_0 > 0.545$. Here, the chaotic attractor undergoes an abrupt instantaneous enlargement to a larger chaotic attractor, which includes the original attractor as a subset, on colliding with a chaotic saddle.

In fact, the present model given by Eq. (6) of a single degree of freedom is very simple and would not be relevant to simulate the proper response of a vehicle. In particular, the model Eq. (6) assumes that the unsprung mass is significantly smaller than the sprung mass. Consequently, the results including the fairly large values of critical excitation amplitudes (where chaotic motion may appear) obtained by numerical simulation cannot be directly compared to experimental results and they can show the behavior of the quarter-car system only qualitatively. Fig. 7 illustrates the deformation of the attractor as F_0 increases. We found that more amplitude of the external excitation is added as F_0 increases, so that the formally simpler periodic orbits are ordered to chaotic trajectories.

5. Conclusion

In this letter, the method of multiple scales is applied to analyze local bifurcation in the quarter-car system with periodically excited road profile. Specially, primary, superharmonic and subharmonic resonance are analyzed. The resulting dimensionless equation of motion for the quarter-car model includes cubic nonlinearities and periodic excitation with asymmetric potential. The model exhibits a variety of interesting phenomena, including resonance and antiresonance phenomena, saddle-node bifurcation, limit cycles, coexistence of multiple solutions, hardening-spring type in the nonlinear resonant frequency response curve for the quarter-car model. The occurrence of resonances may distort the vertical displacement of the model in certain values of the frequency and amplitude of the road profile. This essentially complicate the application of hysteretic nonlinear suspension system to reduce the unwanted vibration in the model. Numerical simulation illustrates

Please cite this article in press as: M. Siewe Siewe, Physics Letters A (2010), doi:10.1016/j.physleta.2010.01.043

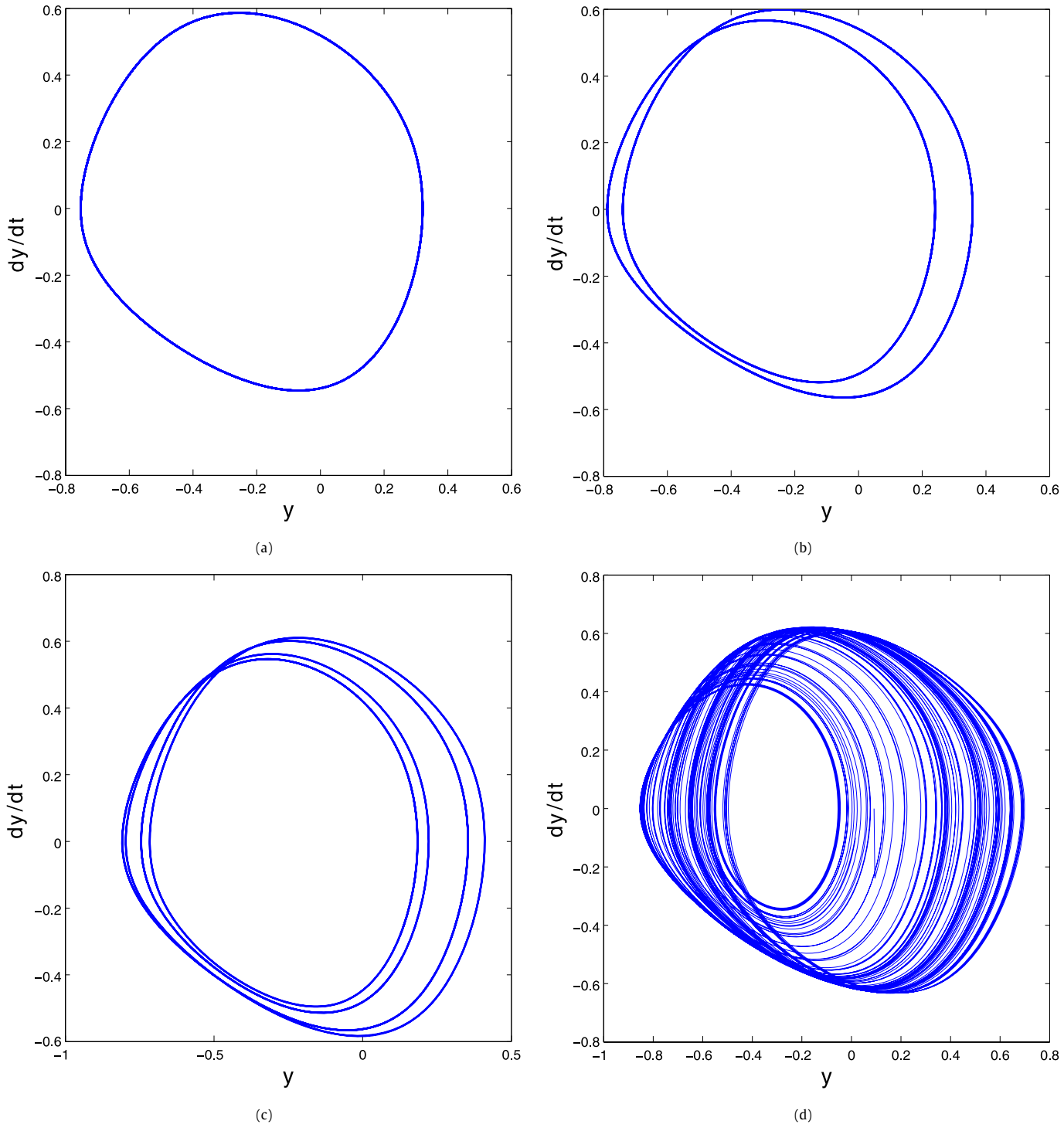

Fig. 7. Phase portraits diagram (a) $F_0 = 0.52$. (b) $F_0 = 0.535$. (c) $F_0 = 0.544$. (d) $F_0 = 0.56$.

that the increase of the amplitude of the external excitation of the road profile transits the system, after the period motion to chaotic motion.

Acknowledgements

The author is grateful to the anonymous referees for their valuable comments. He also indebted to the University of Pretoria for its financial support to do research work as a Postdoctoral Fellow and also indebted to the Department of Mathematics and Applied Mathematics for hosting him to undertake this work.

References

[1] H. Nayfeh, Perturbation Methods, Wiley, New York, 1973.
[2] A.H. Nayfeh, D.T. Mook, Nonlinear Oscillations, Wiley, New York, 1979.
[3] A.H. Nayfeh, Introduction to Perturbation Techniques, Wiley, New York, 1981.
[4] S. Li, S. Yang, W. Guo, Mech. Res. Commun. 31 (2004) 229.
[5] M. Borowiec, G. Litak, M.I. Friswell, Appl. Mech. Mater. 5–6 (2006) 277.
[6] G. Litak, M. Borowiec, M.I. Friswell, K. Szabelski, Commun. Nonlinear Numer. Simul. 13 (2008) 1373.
[7] G. Litak, M. Borowiec, M.I. Friswell, W. Przystupa, Chaos Solitons Fractals 39 (2009) 2448.

[8] R.D. Naik, P.M. Singru, Mech. Res. Commun. 36 (2009) 957.
[9] U. von Wagner, Int. J. Non-Linear Mech. 39 (2004) 753.
[10] J.M.T. Thompson, P. Holmes, Nonlinear Dynamics and Chaos, Wiley, New York, 1987.
[11] F.C. Moon, Chaotic Vibrations, Wiley, New York, 1987.
[12] J. Guckenheimer, P. Holmes, Nonlinear Oscillations, Dynamical Systems, and Bifurcations of Vector Fields, Springer, New York, 1983.
[13] A.H. Nayfeh, N. Balachandran, Applied Nonlinear Dynamics, Wiley, New York, 1995.
[14] A. Andronov, A. Vitt, Zur. Arch. Elektrotech. 24 (1930) 99.

Please cite this article in press as: M. Siewe Siewe, Physics Letters A (2010), doi:10.1016/j.physleta.2010.01.043